

Auger width and branching ratios for Be-like $1s2s^22p^3P^o$ and $1s2s2p^2^3S,^3P,^3D$ resonances and photoionization of Be from $1s^22s2p^3P^o$

Shi-Hsin Lin,¹ Chen-Shiung Hsue,¹ and Kwong T. Chung²¹*Department of Physics, National Tsing-Hua University, Hsin-Chu, Taiwan, Republic of China*²*Department of Physics, North Carolina State University, Raleigh, North Carolina 27607*

(Received 17 December 2000; published 7 June 2001)

The energy and Auger width for the singly core-excited Be-like $1s2s^22p^3P^o$, $(1s2s)^3S,2p^2^3P$, $(1s2s)^1S,2p^2^3P$, and $1s2s2p^2^3S^3D$ states are calculated using a saddle-point complex-rotation method. The decay branching ratios of these states are calculated to check the spin-alignment-dependent Auger decay theory recently proposed by Chung. These branching ratios also enable us to make many positive identifications in the observed Auger spectra. In addition, the photoionization cross section (PICS) from the Be $1s^22s2p^3P^o$ state is calculated for photon energies from 30 eV to 125 eV, including the resonance region. Accurate initial and final state wave functions are used. We find that although the Auger width of the $(1s2s)^3S,2p^2^3P$ transition is smaller than that of $(1s2s)^1S,2p^2^3P$ by a factor of 2.5, its peak PICS is larger by a factor of more than 300.

DOI: 10.1103/PhysRevA.64.012709

PACS number(s): 31.25.Jf, 31.15.Ar, 32.80.Hd, 32.70.Fw

I. INTRODUCTION

Many experimental results on the $1s$ core-excited four-electron resonances from ion-atom or ion-molecule collision experiments [1–11] have been reported in the literature. Although the Auger spectra of lithiumlike systems have been well studied, the Auger spectra of berylliumlike systems are more difficult to identify due to the lack of accurate theoretical data and the multichannel nature of the Auger transitions. There have been a number of theoretical methods that have been successful in studying three-electron systems, e.g., the close-coupling method [12], matrix variation method [13], and quasiprojection operator method [14], etc. In the case of $1s$ core-excited four-electron resonances, theoretical studies are mostly done for photoionization of Be from the $1s^22s^2$ state [15,16]. The final states are of $^1P^o$ symmetry. A recent study has shown that the $^3P^o$ final states could also be important due to the relativistic effect [17]. Unlike the dipole selection rule in photoionization experiments, many resonances of different symmetry are present in collision experiments. The resulting resonance spectra are much more complicated. In this case, accurate theoretical data are needed for positive identification of these resonances.

In 1979, a ‘‘saddle-point’’ method [18] was developed to study inner-shell vacancy systems. In this approach spurious solutions are removed by directly building the proper vacancies into the wave function. A maximum-minimum procedure is then used to arrive at an optimized wave function with a relatively compact set of basis functions. The method has been employed extensively and shown to be a highly accurate and rapidly convergent method. The combination of the saddle-point technique with the complex-rotation method allows the inclusion of the open-channel segment explicitly. Thus the width of a resonance and the small ‘‘shift’’ from the saddle-point energy to the true resonance position can be calculated. This has been proved to be an accurate method in predicting resonance energies and lifetimes for atomic systems was two and three electrons [19].

In the past, the application of the saddle-point method for

four-electron systems was limited to the calculation of energy [20–24]. No saddle-point complex-rotation calculation has been carried out for systems with more than three electrons. In view of the highly accurate results obtained in the past, it will be interesting to find out how effective this method is for four-electron systems.

Recently, Chung [25] proposed a spin-alignment-dependent theory for Auger decay branching ratios. He used this theory to explain the branching ratios for the decay of triply excited three-electron systems. It would be interesting to check how this theory works for four-electron systems.

In this work we calculate the energy and Auger width for the triplet states of the singly core-excited Be $1s2s^22p^3P^o$, $(1s2s)^3S,2p^2^3P$, $(1s2s)^1S,2p^2^3P$, and $1s2s2p^2^3S,^3D$ states. These studies are extended from Be to Ne. The photoionization cross section (PICS) from the Be $1s^22s2p^3P^o$ state is also calculated. We compare our results with available experimental data whenever available. Some of the resonances calculated in this work are not yet measured and our results could be useful in identifying these states in future experiments. Section II briefly presents the theories used in our calculation. Section III shows the computational aspect. We present our results and discussion in Sec. IV. Section V is a short conclusion.

II. THEORY

The nonrelativistic Hamiltonian of a four-electron system is given by

$$H_0 = \sum_{i=1}^4 \left(-\frac{1}{2} \nabla_i^2 - \frac{Z}{r_i} \right) + \sum_{i<j}^4 \frac{1}{r_{ij}}. \quad (1)$$

The relativistic corrections will be calculated using first-order perturbation theory. The perturbation potentials considered are

$$H' = H_1 + H_2 + H_3 + H_4 + H_5 \quad (2)$$

with

$$H_1 = -\frac{1}{8c^2} \sum_{i=1}^4 p_i^4 \quad (\text{kinetic energy correction}),$$

$$H_2 = \frac{Z\pi}{2c^2} \sum_{i=1}^4 \delta(r_i) \quad (\text{Darwin term}),$$

$$H_3 = -\frac{\pi}{c^2} \sum_{i<j}^4 [1 + \frac{8}{3} s_i \cdot s_j] \delta(r_{ij}) \quad (e-e \text{ contact term}),$$

$$H_4 = -\frac{1}{M} \sum_{i<j}^4 \nabla_i \cdot \nabla_j \quad (\text{mass polarization}),$$

$$H_5 = -\frac{1}{2c^2} \sum_{i<j}^4 \frac{1}{r_{ij}} \left[\mathbf{p}_i \cdot \mathbf{p}_j + \frac{r_{ij}(\mathbf{r}_{ij} \cdot \mathbf{p}_i) \cdot \mathbf{p}_j}{r_{ij}^2} \right]$$

(retardation potential),

where M is the mass of the nucleus and $c=137.036$ is the velocity of light.

The LS coupling scheme is used. The basis function is a product of Slater orbitals with angular and spin parts that are the eigenfunctions of L^2, S^2, L_z, S_z ,

$$\Phi_{n_i, l_i}(r_1, r_2, r_3, r_4) = \psi_{n_i}(\mathbf{R}) Y_{l_i}^{LM}(\Omega) X_{SS_z}, \quad (3)$$

where

$$\psi_{n_i}(\mathbf{R}) = \prod_{j=1}^4 r_j^{n_j} \exp(-\alpha_j r_j),$$

$$Y_{l_i}^{LM}(\Omega) = \sum_{m_j} \langle l_1 m_1 l_2 m_2 | l_{12} m_{12} \rangle \langle l_{12} m_{12} l_3 m_3 | l_{123} m_{123} \rangle \\ \times \langle l_{123} m_{123} l_4 m_4 | LM \rangle \prod_{j=1}^4 Y_{l_j m_j}(\Omega_j).$$

l_i represents the set of $l_1, l_2, l_3, l_4, l_{12}, l_{123}$ quantum numbers

$$l_i = [(l_1, l_2) l_{12}, l_3] l_{123}, l_4. \quad (4)$$

The spin angular function can be represented by

$$X_{SS_z} = [(s_1, s_2) S_{12}, s_3] S_{123}, s_4. \quad (5)$$

Three spin angular functions are possible for a triplet,

$$X^1 = [(\frac{1}{2}, \frac{1}{2}) 0, \frac{1}{2}] \frac{1}{2}, \frac{1}{2}, \\ X^2 = [(\frac{1}{2}, \frac{1}{2}) 1, \frac{1}{2}] \frac{1}{2}, \frac{1}{2}, \\ X^3 = [(\frac{1}{2}, \frac{1}{2}) 1, \frac{1}{2}] \frac{1}{2}, \frac{1}{2}. \quad (6)$$

In this work, the Feshbach resonances are obtained by the following procedures.

(1) The energy and the wave function of a closed-channel resonance are first calculated with the saddle-point varia-

tional method [18] for the nonrelativistic Hamiltonian. This wave function is used to calculate the relativistic corrections.

(2) The restricted variation method [26] is used to saturate the functional space to further improve the nonrelativistic energy.

(3) The energy shift due to the interaction with the open channels, the Auger decay width, and the PICS are calculated using the complex-rotation method [27–30].

For example, for $1s 2l2l'2l''$, a $1s$ vacancy is built into the total wave function,

$$\Psi_{LSMS_z} = A \sum_{l_i, n_i} C_{n_i, l_i} (1 - P_j) \psi_{n_i} Y_{l_i}^{LM} X_{SS_z}, \quad (7)$$

where

$$P_j = |\phi_{1s}(r_j)\rangle \langle \phi_{1s}(r_j)|.$$

This vacancy orbital is given by

$$\phi_{1s}(\mathbf{r}) = 2q^{3/2} e^{-qr} Y_{00}(\theta, \phi). \quad (8)$$

The coefficients C and the energy are determined by solving the secular equation

$$\delta \langle H_0 \rangle = \delta \frac{\langle \Psi | H_0 | \Psi \rangle}{\langle \Psi | \Psi \rangle}. \quad (9)$$

The energy is maximized with respect to q and minimized with respect to the α 's. The perturbation correction is obtained from first-order perturbation theory:

$$\Delta E_{rel} = \langle \Psi | H' | \Psi \rangle. \quad (10)$$

The width and the energy shift due to interaction with the open channel are calculated by the complex-rotation method. The photoionization cross section from the Be $1s^2 2s 2p^3 P^o$ state is also calculated with this method in the dipole approximation. We follow closely the procedures used by Chung [31], where a highly accurate PICS was obtained using a method suggested by Rescigno and McKoy [32]. The PICS is given by

$$\sigma(\omega) = \frac{4\pi^2}{3c} \omega \sum_{E_f = E_0 + \omega} |\langle \Psi_0 | \mathbf{D} | \Psi_f \rangle|^2, \quad (11)$$

where ω is the photon energy, \mathbf{D} is the dipole operator, Ψ_0 is the initial ground state wave function, and Ψ_f is the final state wave function.

The polarizability of an atomic system is given by

$$\alpha(\omega) = \left(\sum_n \frac{|\langle \psi_0 | \mathbf{D} | \Psi_n \rangle|^2}{E_n - E_0 - \omega} + \int \frac{|\langle \psi_0 | \mathbf{D} | \Psi_E \rangle|^2}{E - E_0 - \omega - i\epsilon} dE \right. \\ \left. + \sum_n \frac{|\langle \psi_0 | \mathbf{D} | \Psi_n \rangle|^2}{E_n - E_0 + \omega} \right) / 3. \quad (12)$$

Defining

$$\alpha_{-}(\omega) = \left(\sum_n \frac{|\langle \psi_0 | \mathbf{D} | \Psi_n \rangle|^2}{E_n - E_0 - \omega} + \int \frac{|\langle \psi_0 | \mathbf{D} | \Psi_E \rangle|^2}{E - E_0 - \omega - i\epsilon} dE \right) / 3, \quad (13)$$

then

$$\text{Im } \alpha_{-}(\omega) = \frac{1}{3} \pi |\langle \Psi_0 | \mathbf{D} | \Psi_f(E = E_0 + \omega) \rangle|^2. \quad (14)$$

That is,

$$\sigma(\omega) = 4\pi\omega \text{Im } \alpha_{-}(\omega)/c. \quad (15)$$

$\alpha_{-}(\omega)$ is obtained by first constructing a functional [33],

$$F = \langle \Psi_E | H_0 - E_i - \omega | \Psi_E \rangle + \langle \Psi_0 | D | \Psi_E \rangle + \langle \Psi_E | D | \Psi_0 \rangle. \quad (16)$$

Ψ_E is then solved by finding the extremum for F after the complex scaling is done on Ψ_E . Finally, $\alpha_{-}(\omega)$ is given by the expression

$$\alpha_{-}(\omega) = \langle \Psi_E | D | \Psi_0 \rangle / 3. \quad (17)$$

III. COMPUTATIONAL ASPECT

The method of calculating the nonrelativistic energies for these resonances follows closely that of Chung [20]. From 30 to 42 angular spin partial waves were used for most of the resonances considered in this work. For each partial wave, a set of four radial nonlinear parameters is adopted for the four Slater orbitals. These nonlinear parameters are individually optimized in the variation process. Over 200–300 linear parameters are used for the resonances considered in this work. As an example, we list the wave functions and the energy breakdowns for the nitrogen $1s2s2p^2\ ^3D$ state in Table I. In this case, a 302-term wave function is used. The optimized value of the parameter q in Eq. (8) is 5.73.

The relativistic and mass polarization corrections to the energy are calculated using first-order perturbation theory. The relativistic perturbation corrections increase monotonically from 0.05 eV for Be to 2.6 eV for Ne. Even though Be is a system with small Z , the relativistic perturbation corrections for these core-excited resonances are about 0.05 eV, which is about the error bar of the experimental data reported in recent literature. The relativistic corrections for the three-electron target states are much larger. Hence, they could affect the identification of the spectra. Most of the corrections come from the correction to the kinetic energy (H_1) and the Darwin term (H_2). As an example, the results for the nitrogen $1s2s2p^2\ ^3D$ state are listed in Table II. The mass polarization calculations are carried out using ^9Be , ^{11}B , ^{12}C , ^{14}N , ^{16}O , ^{19}F , and ^{20}Ne . The expectation values of the mass polarization effect (H_4) and the retardation effect (H_5) are usually opposite in sign.

In Table III, we list the energies for all the states calculated in this work. The nonlinear parameter q , the nonrelativistic energies calculated with the saddle-point method, the energy shift due to the interaction with open channels, the

perturbation corrections considered in Sec. II, and the energy improvements from the restricted variation method [26] are listed in this table. To a certain extent, q represents the effective nuclear charge experienced by the vacancy. In our computation for core-excited states, several q values are less than $(Z-1)$, rather than the expected values of about $(Z-0.5)$. This implies that the p electrons of the atom are pulled in by the strong nuclear charge so that the effective nuclear charge experienced by the $1s$ vacancy is significantly shielded by the p electrons in addition to the other $1s$ electron. This effect becomes much more apparent for systems with larger Z . Take the $1s2s2p^2\ ^3D$ states as an example; the q values are 3.30, 4.09, 4.92, 5.73, 6.55, and 7.37 for ions with $Z=4, 5, 6, 7, 8, 9$, and 10 respectively. That is, the effective shielding of nuclear charges is 0.70, 0.91, 1.08, 1.27, 1.45, and 1.63 for $Z=4, 5, 6, 7, 8, 9$, and 10, respectively.

IV. RESULTS AND DISCUSSION

Our results for the Auger energies from the four-electron core-excited triplet states will be presented and compared with available experiments in different subsections. In Tables IV and V, we list the calculated energies, total widths, and branching ratios for the Auger transition channels for Be I, B II, C III, N IV, O V, and Ne VII. To compute the Auger energies, we need the energies of the $1s^22s$, $1s^22p$, and $1s^23p$ states of the residual ions. We use the data of Chung [34] for $1s^22s$, of Chung and Zhu [26] for $1s^22p$, and of Wang, Zhu, and Chung [35] for $1s^23p$. These values are listed in Table VI. These data are highly accurate. For example, for Be, the $1s^22s-1s^22p$ energy difference is 3.955 eV, which agrees with the value 3.960 eV given by Bashkin and Stoner [36]. For C, the energy difference is 5.994 eV, which agrees very well with the 5.999 eV from Ref. [36]. For N, the energy difference is 8.000 eV, which compares well with the 8.005 eV from experiment [36]. And finally, for O, the $1s^22s-1s^22p$ energy in this work is 11.992 eV, which agrees well with the value 11.999 eV in Ref. [36].

Recently Chung [25] used a spin-alignment-dependent theory to explain the relative magnitude of the Auger branching ratios. It is interesting to check this theory with our calculated branching ratios. In Table VII we list the relevant spin alignments for the decay channels calculated in this work. Consider the decay of the $^3P^o$ states. For the $a1$ channels, the $2s$ electron number 2 jumps into $1s$ and kicks out electron number 4 in the $2p$ orbital; this occurs due to the $2s2p$ interaction. In the decay channel $a2$, the $2s$ electron number 2 drops to $1s$ and kicks out electron number 3, which is also in the $2s$ orbital. Since the overlap between the two $2s$ electrons is much larger, this explains why the branching ratios of the $a2$ channels are much larger than those in the $a1$ channel. Notice that the ratio decreases monotonically from 74:23 for the Be atom to 64:32 for Ne. This shows that the effect is decreased as the nuclear charge increases, since the electrons are getting closer to the nucleus and to each other. A similar effect can be seen in the branching ratios for the $c1$ channels as compared with the $c2$ channels. For 3S , the decay is somewhat complicated due to the

TABLE I. Energy ($-E$ in $\mu\text{a.u.}$) and wave functions of $1s2s2p^2\ ^3D$ of N. $q=5.73$. a, b, c represent the spin configuration; see Eq. (6). n is the number of linear parameters in the partial wave. $\alpha_1, \alpha_2, \alpha_3,$ and α_4 are the corresponding nonlinear parameters.

$l_1l_2l_3l_4$			Energy	Nonlinear parameters				Subtotal
				α_1	α_2	α_3	α_4	
0011b	01	45	35645443.43	6.9585	3.2580	3.3075	3.6881	35645443.43
0011c	01	22	53371.24	6.8138	3.5000	4.8567	2.7431	35698814.67
0011a	01	8	2654.25	6.8904	2.9660	3.2499	2.7055	35701468.92
0002b	00	23	13235.03	6.7078	2.2233	4.3950	5.0058	35714703.95
0002c	00	7	1203.89	7.0090	2.1673	4.4177	3.2918	35715907.83
0002a	00	7	766.47	7.0388	2.7386	2.9661	2.4101	35716674.31
0112c	11	21	22956.23	6.8692	2.9169	3.6721	3.4943	35739630.53
0112a	11	11	2355.50	6.8436	2.6083	3.0863	3.8389	35741986.03
0112a	11	4	265.69	1.5634	2.7853	4.5765	6.7703	35742251.72
0123c	11	5	704.26	7.3806	2.8914	3.4450	2.6645	35742955.98
0013c	01	11	3926.84	6.7275	2.3250	2.9716	4.4052	35746882.82
0013b	01	4	879.85	6.9031	2.4456	3.5588	3.9806	35747762.67
0013a	01	1	51.70	7.1332	1.8922	2.5688	3.3989	35747814.37
0024b	02	4	198.32	7.0254	1.8636	5.0442	4.8606	35748012.69
0024c	02	4	506.24	7.0206	1.9157	4.9061	4.6789	35748518.93
0035c	03	4	152.85	6.6517	1.7615	6.1171	5.7106	35748671.79
0022b	02	14	5231.13	6.8923	2.5844	4.0222	3.6825	35753902.91
0022b	02	3	105.95	2.0488	6.8941	4.1930	4.6267	35754008.86
0033b	03	3	460.87	6.9924	2.7713	4.5162	4.6029	35754469.73
0121b	11	11	1732.14	2.5026	8.2313	6.4418	2.7275	35756201.87
0121b	11	5	70.41	6.8038	3.4261	3.6242	2.6672	35756272.28
0121c	11	11	1228.72	2.2278	8.5974	6.4227	2.5266	35757501.01
0121c	12	5	180.06	7.2256	2.7193	2.4920	3.5729	35757681.07
0121a	11	5	743.29	6.8473	2.6571	3.7082	3.3058	35758424.36
0121a	11	1	84.14	1.5895	3.9649	7.8795	3.0706	35758508.50
1001a	11	11	952.26	2.5712	2.2679	6.3899	3.8397	35759460.76
0110a	12	4	741.87	6.0316	2.5234	2.7258	3.2580	35760202.63
0110b	12	4	280.12	7.1522	3.2084	2.3986	2.9206	35760482.75
1111b	01	6	856.91	5.3785	5.1364	2.5608	3.6332	35761339.67
0231a	21	5	238.08	7.1546	4.5222	3.5849	2.6998	35761577.74
0231b	21	11	1054.71	6.4588	4.4720	5.2949	2.7851	35762632.46
0231b	21	5	233.04	1.7117	10.5645	7.4856	2.7451	35762865.49
0231c	21	1	70.56	1.4586	9.7251	7.5959	2.5636	35762936.05
0231c	21	5	388.58	6.6225	4.6160	4.0404	2.6165	35763324.64
0123c	13	1	57.22	6.9988	2.7888	3.0946	3.4072	35763381.86
0134c	12	5	209.14	7.2534	2.7463	3.5732	6.2939	35763591.00
0134c	13	1	123.89	7.2392	2.7435	4.3203	5.2099	35763714.90
0134c	14	1	102.18	7.2180	2.7316	4.3106	5.1480	35763817.07
0145c	13	1	67.48	7.2517	2.7296	5.3251	6.2332	35763884.55
0222a	21	1	87.07	7.0684	3.1332	3.4302	3.3016	35763971.62
0044b	04	1	107.55	7.0234	1.8705	5.6297	5.6535	35764079.17
Total	41	302	35764079.17					35764079.17

large mixing from the $1s2s^23s$ configuration. This also explains why the $b1$ channel is much more significant.

A. Identification of Auger spectra for beryllium

Identification of high resolution Auger spectra of boron and beryllium has been carried out by Chung [20] before.

However, the effects of the open channels and the branching ratios are not included in this earlier study. We repeat the same calculation for the core-excited triplet states of Be with larger basis functions. In this work, we use the restricted variation method to saturate the basis functions for the wave function. Furthermore, we use the complex-rotation method to calculate the width and the branching ratios for the decay

TABLE II. The energy of nitrogen $1s2s2p^2\ ^3D$ (in a.u.), including those perturbations considered in Sec II. ΔE_{RV} is the improvement from the restricted variation method, and ΔE_{sh} is the shift due to the interaction with open channels.

Mass polarization	-0.000083
Kinetic energy correction and Darwin term	-0.020702
$e-e$ contact	0.000056
Orbit-orbit interaction	0.000226
Total correction	-0.020503
Subtotal energy	-35.784582
ΔE_{RV}	-0.000621
ΔE_{sh}	0.000161
Total energy	-35.785042

modes. In the Be spectrum of Róðbro *et al.* [1], decays from the lithiumlike states have a higher intensity as compared with those from the four-electron states. Using the calculated Auger transitions tabulated in Table IV, we can identify the lines 4, 8, 11, 13, and 15 in the spectrum. The results of our identification for Be are summarized in Table VIII.

Line 4 is reported at 101.02 ± 0.1 eV. Our calculated Auger energy for

$$1s2s2s2p^3\ P^o \rightarrow 1s^22p + e \quad (18)$$

is 101.12 eV. From the calculated branching ratios of Table IV, it appears that this is the main Auger channel. This $^3P^o$ is the lowest $1s\ 2l2l'2l''$ state. An observable line is expected. This identification agrees with the assignment of Chung [20]. It also agrees with the tentative assignment of

TABLE III. Energies for the triplet four-electron systems. q is the nonlinear parameter. E_{sdl} is the energy calculated by the saddle-point method, ΔE_{sh} is the energy shift due to the interaction with open channels, ΔE_{rel} is the total perturbation corrections considered in Sec II, and ΔE_{RV} represents the energy improvement using the restricted variation method (all in a.u.).

Atom	State	q	E_{sdl}	ΔE_{sh}	ΔE_{rel}	ΔE_{RV}	E_{tot}
Be	$1s2s^22p\ ^3P^o$	3.47	-10.463081	0.000065	-0.002059	-0.000279	-10.465354
	$1s2s2p^2\ ^3S$	3.42	-10.257468	0.000130	-0.001979	-0.000640	-10.259957
	$1s2s2p^2\ ^3P(1)$	3.40	-10.323572	0.000560	-0.001920	-0.000414	-10.325346
	$1s2s2p^2\ ^3P(2)$	3.52	-10.198641	0.000053	-0.001884	-0.000682	-10.201154
	$1s2s2p^2\ ^3D$	3.30	-10.315617	0.000123	-0.001978	-0.000467	-10.317939
B	$1s2s^22p\ ^3P^o$	4.47	-17.273852	0.000104	-0.005293	-0.000273	-17.279314
	$1s2s2p^2\ ^3S$	3.99	-16.944436	0.000080	-0.004980	-0.000413	-16.949749
	$1s2s2p^2\ ^3P(1)$	4.40	-17.055213	0.000684	-0.004915	-0.000684	-17.059893
	$1s2s2p^2\ ^3P(2)$	4.52	-16.882169	0.000011	-0.004760	-0.000577	-16.887495
	$1s2s2p^2\ ^3D$	4.09	-17.045306	0.000195	-0.005020	-0.000544	-17.050675
C	$1s2s^22p\ ^3P^o$	5.47	-25.836932	0.000015	-0.011440	-0.000336	-25.848693
	$1s2s2p^2\ ^3S$	4.88	-25.393330	0.000097	-0.010677	-0.000513	-25.404423
	$1s2s2p^2\ ^3P(1)$	5.40	-25.537099	0.000756	-0.010593	-0.000449	-25.547385
	$1s2s2p^2\ ^3P(2)$	5.52	-25.323289	0.000013	-0.010253	-0.000605	-25.334134
	$1s2s2p^2\ ^3D$	4.92	-25.528835	0.000148	-0.010770	-0.000587	-25.540044
N	$1s2s^22p\ ^3P^o$	6.47	-36.151042	0.000234	-0.021894	-0.000362	-36.173064
	$1s2s2p^2\ ^3S$	5.74	-35.595413	0.000095	-0.020329	-0.000563	-35.615357
	$1s2s2p^2\ ^3P(1)$	6.40	-35.768964	0.000812	-0.020247	-0.000467	-35.788866
	$1s2s2p^2\ ^3P(2)$	6.52	-35.516662	0.000026	-0.019592	-0.000640	-35.536868
	$1s2s2p^2\ ^3D$	5.73	-35.764079	0.000161	-0.020503	-0.000621	-35.785042
O	$1s2s^22p\ ^3P^o$	7.47	-48.215669	0.000264	-0.038334	-0.000381	-48.254120
	$1s2s2p^2\ ^3S$	6.43	-47.548972	0.000118	-0.035491	-0.000512	-47.584857
	$1s2s2p^2\ ^3P$	7.38	-47.750785	0.000850	-0.035428	-0.000481	-47.785844
	$1s2s2p^2\ ^3D$	6.55	-47.750335	0.000245	-0.035766	-0.000618	-47.786474
F	$1s2s^22p\ ^3P^o$	8.47	-62.030610	0.000263	-0.062720	-0.000394	-62.093461
	$1s2s2p^2\ ^3S$	7.28	-61.253377	0.000118	-0.057941	-0.000552	-61.311752
	$1s2s2p^2\ ^3P$	8.38	-61.482592	0.000895	-0.057918	-0.000491	-61.540106
	$1s2s2p^2\ ^3D$	7.37	-61.487109	0.000169	-0.058368	-0.000658	-61.545966
Ne	$1s2s^22p\ ^3P^o$	9.47	-77.595745	0.000259	-0.097297	-0.000405	-77.693188
	$1s2s2p^2\ ^3S$	8.21	-76.708351	0.000120	-0.089735	-0.000585	-76.798551
	$1s2s2p^2\ ^3P$	9.37	-76.964361	0.000901	-0.089755	-0.000498	-77.053713
	$1s2s2p^2\ ^3D$	8.19	-76.974264	0.000297	-0.090346	-0.000671	-77.064984

TABLE IV. Auger energy (E_{Au}), branching ratio (BR), and Auger width (Γ) for Be I, B II, and C IV. 1 a.u. = 27.20974 eV.

Atom	State	Channel	BR	E_{Au} (eV)	Γ (meV)
Be I	$1s2s^22p^3P^o$	$1s^22s+kp$	23.9%	105.07	40.6
		$1s^22p+ks$	73.9%	101.12	
		$1s^22p+kd$	2.2%	101.12	
	$1s2s2p^2^3S$	$1s^22s+ks$	95.9%	110.66	13.7
		$1s^22p+kp$	4.1%	106.71	
	$1s2s2p^2^3P(1)$	$1s^22p+kp$	$\sim 100\%$	104.93	7.3
		$1s^23p+kp$			
	$1s2s2p^2^3P(2)$	$1s^22p+kp$	$\sim 100\%$	108.31	18.4
		$1s^23p+kp$			
	$1s2s2p^2^3D$	$1s^22s+kd$	90.2%	109.08	14.8
		$1s^22p+kp$	9.8%	105.13	
	B II	$1s2s^22p^3P^o$	$1s^22s+kp$	27.5%	167.38
$1s^22p+ks$			69.9%	161.38	
$1s^22p+kd$			2.6%	161.38	
$1s2s2p^2^3S$		$1s^22s+ks$	83.6%	176.34	17.7
		$1s^22p+kp$	16.4%	170.35	
$1s2s2p^2^3P(1)$		$1s^22p+kp$	$\sim 100\%$	167.35	9.82
		$1s^23p+kp$			
$1s2s2p^2^3P(2)$		$1s^22p+kp$	$\sim 100\%$	172.03	33.3
		$1s^23p+kp$			
$1s2s2p^2^3D$		$1s^22s+kd$	89.1%	173.60	32.22
		$1s^22p+kp$	10.9%	167.60	
C IV		$1s2s^22p^3P^o$	$1s^22s+kp$	29.5%	243.27
	$1s^22p+ks$		67.1%	235.27	
	$1s^22p+kd$		2.9%	235.27	
	$1s2s2p^2^3S$	$1s^22s+ks$	79.8%	255.36	23.5
		$1s^22p+kp$	20.2%	247.36	
	$1s2s2p^2^3P(1)$	$1s^22p+kp$	$\sim 100\%$	243.47	10.2
		$1s^23p+kp$			
	$1s2s2p^2^3P(2)$	$1s^22p+kp$	$\sim 100\%$	249.27	45.2
		$1s^23p+kp$			
	$1s2s2p^2^3D$	$1s^22s+kd$	88.6%	251.67	48.5
		$1s^22p+kp$	11.4%	243.67	

Ródbro *et al.* [1], which was based on the calculation of Safronova and Kharitonova [37] at 101.4 eV.

Among the four-electron lines, line 8 is a line of significant intensity. The reported line position is at 104.88 ± 0.1 eV. We identify this line as the transition

$$1s2s2p^2^3P(1) \rightarrow 1s^22p + e. \quad (19)$$

Our calculated energy is 104.93 eV which agrees with the value 104.91 eV obtain by Chung [20]. As can be seen from Table IV, this is a preferred decay mode since the $1s^22s$ channel is forbidden in the nonrelativistic approximation.

In the assignment of Ródbro *et al.* [1], line 8 at 104.9 eV was identified as the

$$1s2s^22p^3P^o \rightarrow 1s^22s + e \quad (20)$$

TABLE V. Auger energy (E_{Au}), branching ratio (BR), and Auger width (Γ) for N IV, O V, F VI, and Ne VII. 1 a.u. = 27.21033 eV.

Atom	State	Channel	BR	E_{Au} (eV)	Γ (meV)	
N IV	$1s2s^22p^3P^o$	$1s^22s+kp$	30.6%	332.79	79.0	
		$1s^22p+ks$	66.5%	322.80		
		$1s^22p+kd$	2.9%	322.80		
	$1s2s2p^2^3S$	$1s^22s+ks$	78.2%	347.97	28.6	
		$1s^22p+kp$	21.8%	337.97		
	$1s2s2p^2^3P(1)$	$1s^22p+kp$	$\sim 100\%$	333.25	10.8	
		$1s^23p+kp$				
	$1s2s2p^2^3P(2)$	$1s^22p+kp$	$\sim 100\%$	340.11	55.0	
		$1s^23p+kp$				
	$1s2s2p^2^3D$	$1s^22s+kd$	88.2%	343.35	57.7	
		$1s^22p+kp$	11.8%	333.36		
		$1s^22p+ks$	65.5%	423.97		
O V	$1s2s^22p^3P^o$	$1s^22s+kp$	31.4%	435.96	86.4	
		$1s^22p+ks$	65.5%	423.97		
		$1s^22p+kd$	3.0%	423.97		
	$1s2s2p^2^3S$	$1s^22s+ks$	77.3%	454.17	32.8	
		$1s^22p+kp$	22.7%	446.18		
	$1s2s2p^2^3P$	$1s^22p+kp$	$\sim 100\%$	436.71	11.5	
		$1s^23p+kp$	%			
	$1s2s2p^2^3D$	$1s^22s+kd$	87.9%	448.68	69.1	
		$1s^22p+kp$	12.1%	436.69		
		$1s^22p+ks$	64.9%	538.79		
	F VI	$1s2s^22p^3P^o$	$1s^22s+kp$	31.9%	552.79	87.6
			$1s^22p+ks$	64.9%	538.79	
$1s^22p+kd$			3.2%	538.79		
$1s2s2p^2^3S$		$1s^22s+ks$	76.7%	574.06	36.2	
		$1s^22p+kp$	23.3%	560.06		
$1s2s2p^2^3P$		$1s^22p+kp$	$\sim 100\%$	553.84	12.1	
		$1s^23p+kp$				
$1s2s2p^2^3D$		$1s^22s+kd$	87.8%	567.68	72.9	
		$1s^22p+kp$	12.2%	552.68		
		$1s^22p+ks$	64.4%	667.27		
Ne VII		$1s2s^22p^3P^o$	$1s^22s+kp$	32.4%	683.30	94.9
			$1s^22p+ks$	64.4%	667.27	
	$1s^22p+kd$		3.2%	667.27		
	$1s2s2p^2^3S$	$1s^22s+ks$	76.2%	707.64	39.2	
		$1s^22p+kp$	23.8%	691.61		
	$1s2s2p^2^3P$	$1s^22p+kp$	$\sim 100\%$	684.67	11.4	
		$1s^23p+kp$				
	$1s2s2p^2^3D$	$1s^22s+kd$	87.7%	700.39	76.7	
		$1s^22p+kp$	12.3%	684.36		
		$1s^22p+ks$	64.4%	667.27		

transition. Our calculated energy for this transition is 105.07 eV. It lies outside the experimental uncertainty. Furthermore, from the branching ratio of Table IV, we know that this is not the main decay channel for $1s2s^22p^3P^o$. Since the main decay channel yields only a weak line (line 4), this transition cannot be the main contributor to line 8, which is a line with significant intensity. This conclusion was already presented by Chung based on the decay branching ratios of O V [9]. Our explicit calculation confirms this conclusion.

Lines 11 is weak but broad. The reported position is 107.02 ± 0.2 eV. Chung [20] claims this is the result of a blend of

TABLE VI. Energies (in eV) used for the three-electron target states.

	$1s^22s$	$1s^22p$	$1s^23p$	$1s^22s-1s^22p$	
				This work	Expt. ^a
Be	-14.3268967	-14.1815456	-13.8871577	3.955 eV	3.960 eV
B	-23.4306217	-23.2103335	-22.5513433	5.994 eV	5.999 eV
C	-34.7890742	-34.495071	-33.3305756	8.000 eV	8.005 eV
N	-48.4034966	-48.036188	-46.2261927	3.955 eV	3.960 eV
O	-64.2758399	-63.835141	-61.2400335	11.992 eV	11.999 eV
F	-82.4085547	-81.894024	-78.3743389		
Ne	-102.8045041	-102.215427	-97.6316979		

^aReference [36].

$$1s2s2p^2\ ^3S \rightarrow 1s^22p + e \quad (21)$$

and

$$1s2s2p^2\ ^1D \rightarrow 1s^22p + e. \quad (22)$$

In this work, our prediction for transition (21) is at 106.71 eV. This result agrees with that of Ref. [20] at 106.76 eV.

Lines 14 and 15 are so close that it is difficult to resolve them experimentally. Of the states we considered in this work, the transition within this range is

$$1s2s2p^2\ ^3D \rightarrow 1s^22s + e. \quad (23)$$

The transition energy is calculated to be 109.08 eV. It lies within the error bar of line 15, 109.26 ± 0.2 eV.

We identify the line 16 reported at 110.61 ± 0.2 eV as the transition

$$1s2s2p^2\ ^3S \rightarrow 1s^22s + e, \quad (24)$$

predicted at 110.66 eV. According to the calculated branching ratio, 96% (see Table IV), this is the main decay channel for the Be $1s2s2p^2\ ^3S$ state. Our prediction agrees very well with the experiment. This line was tentatively assigned as the transition from $[(1s2s)^3S3s]^2S$ in Ref. [1] and was not discussed by Chung [20].

B. Identification of Auger spectra for B II

In the boron spectrum of Rodbro *et al.* [1], the lithiumlike lines are unambiguously identified [38]. Although these lines appear to have a higher intensity as compared with the four-electron spectral lines, the lines 9, 15, 16, and 18 are also of very significant intensity. In this work, we will identify the lines 3, 9, 12, 14, and 15. These identifications are summarized in Table IX. The calculated energies, branching ratios, and total widths for the Auger transition channels for the triplet resonances of boron are listed in Table IV.

Line 3 is located at 161.24 ± 0.1 eV. This line has been identified as coming from the lithiumlike transition

$$[1s(2s2p)^3P]^2P^o \rightarrow 1s^2 + e. \quad (25)$$

It was predicted to be at 161.26 eV [38]. This is the most intense line in the boron spectrum within the energy range

140–220 eV. There is little doubt that line 3 comes mainly from this $^2P^o$ state. Our calculated electron energy for the transition

$$1s2s^22p\ ^3P^o \rightarrow 1s^22p + e \quad (26)$$

is at 161.38 eV in very good agreement with the value 161.36 eV obtained by Chung [20]. As was discussed in [20], since this $^3P^o$ state is the lowest $1s\ 2l2l'2l''$ state, a significant amount of it could be present in the collision product. Hence, it is possible that this transition also contributes to the observed 161.24 ± 0.1 eV line.

Line 9 is one of the most intense lines in the boron spectrum. Its position is reported at 167.34 ± 0.2 eV. In this work, there are two transitions lying within this energy range:

$$1s2s2p^2\ ^3P(1) \rightarrow 1s^22p + e, \quad (27)$$

predicted at 167.35 eV, and

TABLE VII. Electron spin alignment for the relevant Auger transition channels considered.

	Electron orbitals			Decay channel
	$1s$	$2s^2$	$2p$	
$a1$	\uparrow	$\downarrow\uparrow$	\uparrow	$^3P^o \rightarrow 1s^22s + e$
	1	2,3	4	
$a2$	\uparrow	$\downarrow\uparrow$	\uparrow	$^3P^o \rightarrow 1s^22p + e$
	1	2,3	4	
$b1$	\uparrow	\uparrow	$\downarrow\uparrow$	$^3S \rightarrow 1s^22s + e$
	1	2	3,4	
$b2$	\uparrow	\uparrow	$\downarrow\uparrow$	$^3S \rightarrow 1s^22p + e$
	1	2	3,4	
$c1$	\uparrow	\uparrow	$\downarrow\uparrow$	$^3D \rightarrow 1s^22s + e$
	1	2	3,4	
$c2$	\uparrow	\uparrow	$\downarrow\uparrow$	$^3D \rightarrow 1s^22p + e$
	1	2	3,4	

TABLE VIII. Identification of experimental Auger spectra for Be I (in eV).

Line ^b	Experiment ^a this work		Theory		
	Energy	Intensity ^c	This work	Chung ^d	Identification
4	101.02±0.1	weak	101.12	101.10	$1s2s^22p^3P^o \rightarrow 1s^22p+e$
8	104.88±0.1	strong-	104.93	104.91	$1s2s2p^2^3P(1) \rightarrow 1s^22p+e$
			105.07	105.07	$1s2s2p^2^3P^o \rightarrow 1s^22s+e$
			105.13	105.24	$1s2s2p^2^3D \rightarrow 1s^22p+e$
11	107.02±0.2	weak	106.71	106.76	$1s2s2p^2^3S \rightarrow 1s^22p+e$
13	108.15±0.2	median-	108.31	108.37	$1s2s2p^2^3P(2) \rightarrow 1s^22p+e$
15	109.26±0.2	strong(?)	109.08	109.21	$1s2s2p^2^3D \rightarrow 1s^22s+e$
16	110.61±0.2	median-	110.66		$1s2s2p^2^3S \rightarrow 1s^22s+e$

^aRódbro *et al.*, Ref. [1].

^bThis line number is the assignment in Ref. [1].

^cThe intensities of these spectral lines are all comparatively weak. The terms used here are in the relative sense. + (-) indicates the intensity is at the higher (lower) end of the given range.

^dReference [20].

$$1s2s^22p^3P^o \rightarrow 1s^22s+e, \quad (28)$$

predicted at 167.38 eV. These values are in almost complete agreement with the results of Chung, who obtained 167.34 eV and 167.38 eV, respectively. As was discussed in [20], the transition (27) is a symmetry preferred decay, and the predicted energy agrees well with the experiment. It can be seen from the branching ratios in Table IV that the transition (28) is not the major Auger channel. Line 9 mostly comes from the transition (27).

Line 12 located at 170.57±0.2 eV is a weak line. It is somewhat broad, and it was suggested [20] to be a blend of

$$1s2s2p^2^3S \rightarrow 1s^22p+e \quad (29)$$

and

$$1s2s2p^2^1D \rightarrow 1s^22p+e. \quad (30)$$

In this work, the transition energy of (29) is predicted at 170.35 eV in good agreement with the value 170.33 eV in [20]. It is within the error bar of the experiment. The same two transitions also contributed to the blended weak line 11 in the Be Auger spectrum.

Line 14 is reported at 172.22±0.2 eV. Our calculated energy for the transition

$$1s2s2p^2^3P(2) \rightarrow 1s^22p+e \quad (31)$$

is 172.03 eV, in good agreement with 172.05 eV in [20]. This value agrees with the reported 172.22±0.2 eV of line 14.

Line 15 is reported at 173.58±0.2 eV with a strong intensity. In this work, the transition

$$1s2s2p^2^3D \rightarrow 1s^22s+e \quad (32)$$

is predicted at 173.60 eV, as compared with the value 173.72 eV in [20]. From our calculated branching ratio in Table IV,

TABLE IX. Identification of experimental Auger spectra for B II (in eV).

Line ^b	Experiment ^a		Theory		
	Energy	Intensity ^c	This work	Chung ^d	Identification
3	161.24±0.1	strong+	161.38	161.36	$1s2s^22p^3P^o \rightarrow 1s^22p+e$
9	167.34±0.2	strong	167.35	167.34	$1s2s2p^2^3P(1) \rightarrow 1s^22p+e$
			167.38	167.38	$1s2s2p^2^3P^o \rightarrow 1s^22s+e$
			167.60	167.72	$1s2s2p^2^3D \rightarrow 1s^22p+e$
12	170.57±0.2	weak	170.35	170.35	$1s2s2p^2^3S \rightarrow 1s^22p+e$
14	172.22±0.2	median-	172.03	172.05	$1s2s2p^2^3P(2) \rightarrow 1s^22p+e$
15	173.58±0.2	strong	173.60	173.72	$1s2s2p^2^3D \rightarrow 1s^22s+e$
(18)	176.08±0.2	median+	176.34	176.34	$1s2s2p^2^3S \rightarrow 1s^22s+e$

^aRódbro *et al.*, Ref. [1].

^bThis line number is the assignment in the Ref. [1].

^cThe terms used here are in the relative sense. + (-) indicates the intensity is at the higher (lower) end of the given range.

^dReference [20].

TABLE X. Identification of experimental Auger spectra for C IV (in eV).

Line ^a	Experiment		Theory		
	Ref. [3]	Ref. [2]	This work	Other	Identification
3	235.44±0.2	235.1±0.2	235.27	235.43 ^b	$1s2s^22p^3P^o \rightarrow 1s^22p+e$
10	243.38±0.2	242.0±0.2	243.27	243.48 ^b	$1s2s^22p^3P^o \rightarrow 1s^22s+e$
10	243.38±0.2	242.0±0.2	243.47		$1s2s2p^2^3P(1) \rightarrow 1s^22p+e$
			243.67		$1s2s2p^2^3D \rightarrow 1s^22p+e$
13	247.20±0.2		247.36		$1s2s2p^2^3S \rightarrow 1s^22p+e$
15	249.21±0.2	249.1±0.2	249.27		$1s2s2p^2^3P(2) \rightarrow 1s^22p+e$
16	251.48±0.2	251.4±0.2	251.67	252.61 ^b	$1s2s2p^2^3D \rightarrow 1s^22s+e$
19	255.31±0.4	255.2±0.2	255.36		$1s2s2p^2^3S \rightarrow 1s^22s+e$

^aLine number assigned in Ref. [3].

^bUnrestricted Hartree-Fock plus electron-pair correlation energies, Ref. [3].

we find that $1s2s2s^2^3D$ decays mostly through this transition channel, with a branching ratio of about 90%. Hence, it should be present in the existing experimental data for Be, B, C [1], and O [5].

Line 18 is reported at 176.08 ± 0.2 eV. Our calculation shows that the energy of

$$1s2s2p^2^3S \rightarrow 1s^22s+e \quad (33)$$

is predicted at 176.34 eV, in complete agreement with [20]. It is slightly outside the error bar of the reported line. Chung [20] suggests this line is probably the transition

$$1s2p^3^1D^o \rightarrow 1s^22p+e. \quad (34)$$

There may also be some contribution from the transition of (33). Our results support Chung's [20] contention.

C. Identification of Auger spectra for C III

In this subsection we identify the Auger spectrum by Mann [2] and by R odbro *et al.* [1] as recalibrated by Bruch and collaborators [3]. The Auger transition calculated in this work is listed in Table IV. A comparison of the energies of the Auger electrons obtained in this work and in the experiments is summarized in Table X.

The 235.1 ± 0.2 eV line of Mann [2] was identified as coming from the transition

$$1s2s^22p^3P^o \rightarrow 1s^22p+e. \quad (35)$$

Our calculated result, 235.27 eV, agrees with this identification. In [3], line 3 was located at 235.44 ± 0.2 eV and it was also identified as coming from the transition

$$[1s(2s2p)^3P]^2P^o \rightarrow 1s^2+e, \quad (36)$$

whose energy was predicted to be 235.55 eV. Clearly this 235.44 eV line is the overlap of two Auger processes.

Line 10 at 243.38 ± 0.2 eV is the second most intense line in the observation of R odbro *et al.* (see Fig. 1, quoted from Ref. [3]). Our results suggest that this could be the overlap of two Auger channels:

$$1s2s2p^2^3P(1) \rightarrow 1s^22p+e, \quad (37)$$

$$1s2s^22p^3P^o \rightarrow 1s^22s+e. \quad (38)$$

The transition energy of (37) is predicted to be 243.47 eV and lies within the experimental uncertainty. Our calculated energy of (38) is predicted to be 243.27 eV as compared with the unrestricted Hartree-Fock self-consistent field result of 243.48 eV in Ref. [3]. It should be noted from the branching ratio in Table IV that this channel is a less preferred decay mode. There is another transition,

$$1s2s2p^2^3D \rightarrow 1s^22p+e, \quad (39)$$

whose energy is predicted to be 247.36 eV and which could contribute to this line. But the contribution is probably very small.

Line 13 is reported at 247.20 ± 0.2 eV in Ref. [3] with very weak intensity (see Fig. 1). It is not reported in Ref. [2]. Our calculated Auger energy for the transition

$$1s2s2p^2^3S \rightarrow 1s^22p+e \quad (40)$$

is at 247.36 eV, and this is a channel with branching ratio of about 20%.

The most intense line in the spectrum of Ref. [3] is line 16 at 251.48 ± 0.2 eV. It is also reported at 251.48 ± 0.2 eV in Ref. [2]. Chung claims that the reason for this strong intensity is the result of the overlap of several Auger channels [21]. They are

$$1s2s2p^2^1P \rightarrow 1s^22p+e, \quad (41)$$

$$1s2s2p^2^1S \rightarrow 1s^22p+e, \quad (42)$$

and

$$1s2s2p^2^3D \rightarrow 1s^22p+e. \quad (43)$$

In this work, our calculated transition energy of (43) is predicted to be 251.67 eV, which is within the experimental uncertainty. Also, from the branching ratio listed in Table IV, we know that (43) is the major decay channel of the 3D state. This transition is also observed in the existing experiments on Be, B, and O; hence we can confirm part of the claim of Chung.

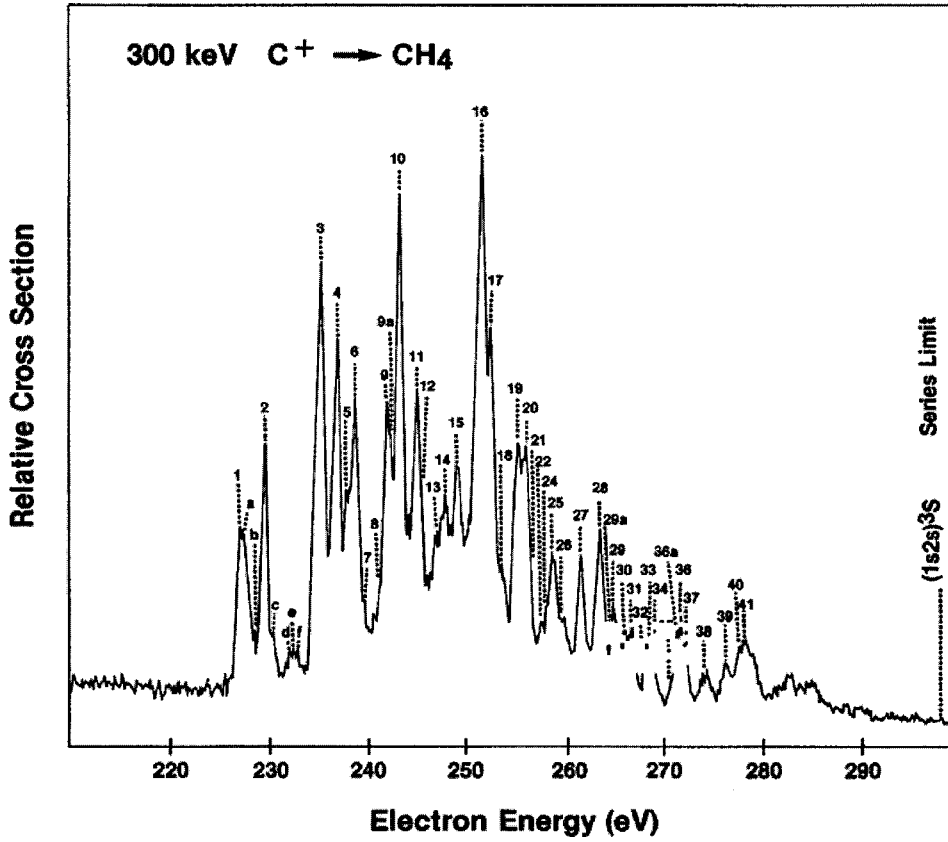


FIG. 1. High resolution *KLL* Auger spectrum of carbon in a single-collision condition (from Ref. [3]).

Line 19 at 255.31 ± 0.4 eV in Ref. [3] is also observed in Ref. [2] at 255.2 ± 0.2 eV. We identify this line as the Auger channel

$$1s2s2p^2\ ^3S \rightarrow 1s^22s + e, \quad (44)$$

which is predicted at 255.36 eV in this work. The agreement with experiment is quite good and it also agrees with the result of Chung [21].

D. Identification of Auger spectra for O v

The transition line

$$1s2s^22p\ ^3P^o \rightarrow 1s^22p + e \quad (45)$$

is embedded in the more intense transition line

$$[1s(2s2p)^3P]^2P^o \rightarrow 1s^2 + e \quad (46)$$

for Be, B, and C. In the experiment [5] of Bruch *et al.*, these two lines are resolved into lines *A3* and *B1* for oxygen; see Fig. 2. The energy of transition (46) is identified as the line *A3* at 425.0 ± 0.2 eV, and the line *B1* is located at 423.9 ± 0.2 eV in Ref. [5]. We can clearly identify the line *B1* as (45) here. Our result for line *B1*, 423.97 eV, agrees better with the experiment than the results of Ref. [8], 424.2 eV, and Ref. [39], 424.54 eV. From our agreement with the experiment, we can make a positive identification for these two lines. The other Auger channel of this $^3P^o$ state

$$1s2s^22p\ ^3P^o \rightarrow 1s^22s + e, \quad (47)$$

predicted at 435.96 eV, could also correspond to the spectral line *B4* in the experiment at 435.9 ± 0.2 eV. This transition line blends with

$$1s2s2p^2\ ^3P(1) \rightarrow 1s^22p + e \quad (48)$$

and

$$1s2s2p^2\ ^3D \rightarrow 1s^22p + e \quad (49)$$

in the discussion of the previous subsections for lower *Z* atoms, Be, B, and C. For oxygen, this Auger spectral line (47) is more separated from the other two lines in the experiment [5]. Thus it can be positively identified as line *B4* in this work.

Perhaps the most detailed experimentally analyzed ($1s2s^22p$) $^3P^o$ resonance is for O v. In 1987, Bruch *et al.* reported an experimental result [9] for partial autoionization rates of O^{4+} ($1s2s^22p$) $^3P^o$ and $^1P^o$. Since we have calculated the branching ratios, we can compare our results with the experimental data. The measured branching ratio of channels (45) to (47) is 1.7 ± 0.1 . In this work, we predict this ratio to be 1.9.

The energies of the transitions (48) and (49) are close in our calculation. The transition line (48) is predicted at 436.71 eV, and (49) is predicted at 436.69 eV. The predicted energies are so close that it will be very difficult to resolve them experimentally. There is a line *B5* at 436.6 ± 0.2 eV which was identified as (48) in Ref. [5]. Our results suggest that (49) could also have contributed to this line.

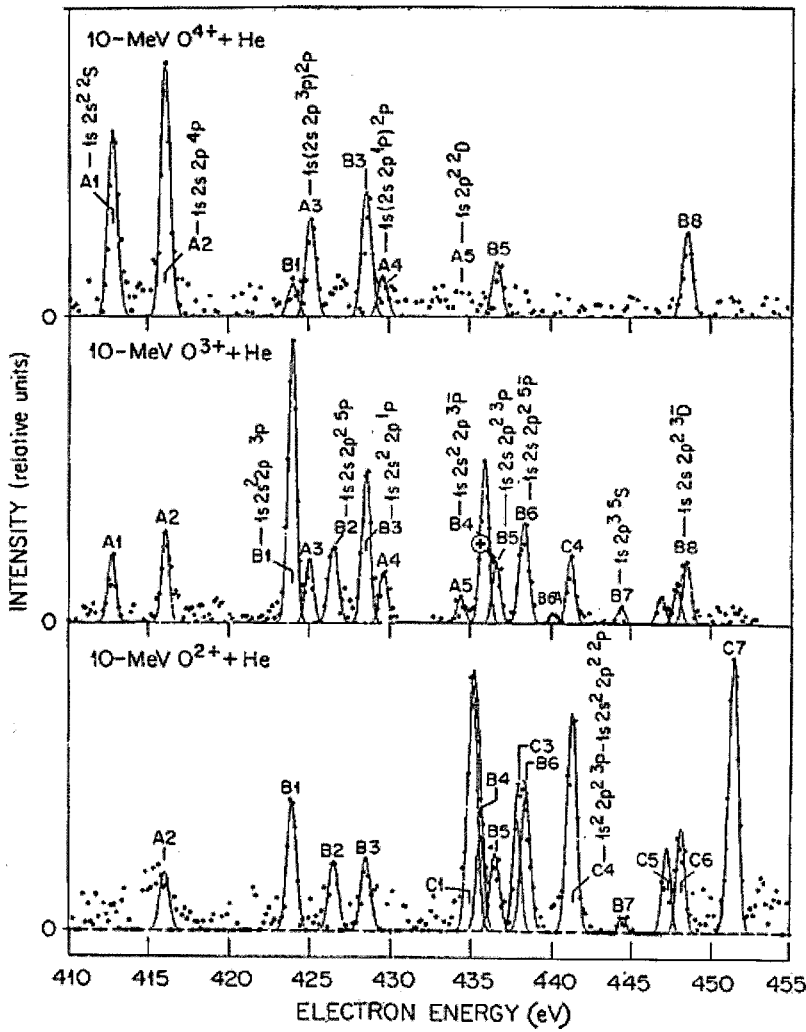


FIG. 2. High resolution K Auger spectra from 10-MeV O^{n+} ($n=4, 3$, and 2) projectiles colliding with He atoms. Background has been subtracted and electron energies have been transformed to the projectile rest frame. (From Ref. [5].)

We also list the experimental results of Ref. [8] in Table XI. The resolution of this experiment is lower than that of the experiment of Ref. [5]. Since the spacing between those resonances [5] is smaller than the error bar of the experiment [8], we cannot positively identify those lines in Ref. [8]. Here we just list them for reference. For line 4 of Ref. [8] at 443 ± 2 eV, the transition could be

$$1s2s2p^2\ ^3S \rightarrow 1s^22p + e. \quad (50)$$

This transition is predicted to be at 442.5 eV, 442.97 eV, and 442.18 eV in Ref. [8], Ref. [39], and this work, respectively. Line 6 at 454 ± 1 eV could be from

$$1s2s2p^2\ ^3S \rightarrow 1s^22s + e, \quad (51)$$

predicted at 454.17 eV in this work.

TABLE XI. Identification of experimental Auger spectra for O v (in eV).

Experiment ^a		Theoretical results			
Line ^b	Energy	Ref. [8]	Ref. [39]	This work	Identification
B1	423.9 ± 0.2	424.2	424.54	423.97	$1s2s^22p\ ^3P^o \rightarrow 1s^22p + e$
B4	435.9 ± 0.2	436.2	436.63	435.96	$1s2s2p^2\ ^3P^o \rightarrow 1s^22s + e$
B5	436.6 ± 0.2	436.4	436.66	436.71	$1s2s2p^2\ ^3P(1) \rightarrow 1s^22p + e$
		437.0	437.66	436.69	$1s2s2p^2\ ^3D \rightarrow 1s^22p + e$
4 ^c	443 ± 2	442.5	442.97	442.18	$1s2s2p^2\ ^3S \rightarrow 1s^22p + e$
B8	449.0	449.74	448.68	448.68	$1s2s2p^2\ ^3D \rightarrow 1s^22s + e$
6 ^c	454 ± 1	454.5	455.06	454.17	$1s2s2p^2\ ^3S \rightarrow 1s^22s + e$

^aBruch *et al.* [5].

^bLine number assigned in Ref. [5].

^cReference [8].

TABLE XII. Identification of experimental Auger spectra for Ne VII (in eV).

Line ^b	Experiment ^a		Theory		Identification		
	Energy	Other work	This work				
B3	667.3±0.2 ^a	667.27 ^c	667.27		1s2s2p ³ P ^o →1s ² 2p+e		
	666.88 ^d	666.95 ^e					
	665±1 ^f	667.83 ^g 667.8 ^f					
B6	683.2±0.1	683.295 ^c	683.30		1s2s2p ² 3P ^o →1s ² 2s+e		
	683±1 ^f	682.97 ^e					
	683.05 ^d	683.8 ^f					
A5	684.0±0.4	683.99 ^e 684.4 ^f 685.28 ^d	684.36		1s2s2p ² 3D→1s ² 2p+e		
A5	684.0±0.4	684.28 ^e 684.57 ^d	684.67		1s2s2p ² 3P(1)→1s ² 2p+e		
		691.575 ^e				691.61	1s2s2p ² 3S→1s ² 2p+e
		692.34 ^g					
B10	699.8±0.4	700.24 ^e 701.42 ^g 707.60 ^e 708.47 ^g	700.39		1s2s2p ² 3D→1s ² 2s+e		
			707.64		1s2s2p ² 3S→1s ² 2s+e		

^aReference [7].^bLine number assigned in Ref. [7].^cSaddle-point method including relativistic corrections, Ref. [7].^dKádár *et al.* [11].^e1/Z expansion, Ref. [7] and the references in Ref. [7].^fSchumann *et al.* [42].^gMulticonfiguration Dirac-Fock calculations, Ref. [7].

E. Identification of Auger spectra for Ne VII

In the experiment of Bruch *et al.* [7], line B3 is the most intense line located at 667.3 ± 0.2 eV. It agrees very well with the 667.27 eV predicted for channel

$$1s2s^22p^3P^o \rightarrow 1s^22p+e \quad (52)$$

in this work. Our result also agrees with the theoretical result in Ref. [7] (see Table XII). This is the most intense line in the 100-MeV Ne⁵⁺+He collision spectrum (Fig. 3).

The next major peak, B6, at 683.2 ± 0.1 eV is identified as coming from the Auger channel:

$$1s2s^22p^3P^o \rightarrow 1s^22s+e. \quad (53)$$

Our calculated result for (53) is 683.30 eV, in agreement with the experiment. It also agrees with the theoretical result of the saddle-point method, 683.295 eV, in Ref. [7]. B3 and B6 are the two most intense lines in the observed Ne⁵⁺+He spectrum [7]. The intensity ratio of the spectral lines appears to agree excellently with the branching ratios calculated in this work. Hence, we have positively identified the two most intense lines in the observed spectrum of Bruch *et al.* [7]. We note, however, that our results are slightly higher than the observed data of Kádár *et al.* [11].

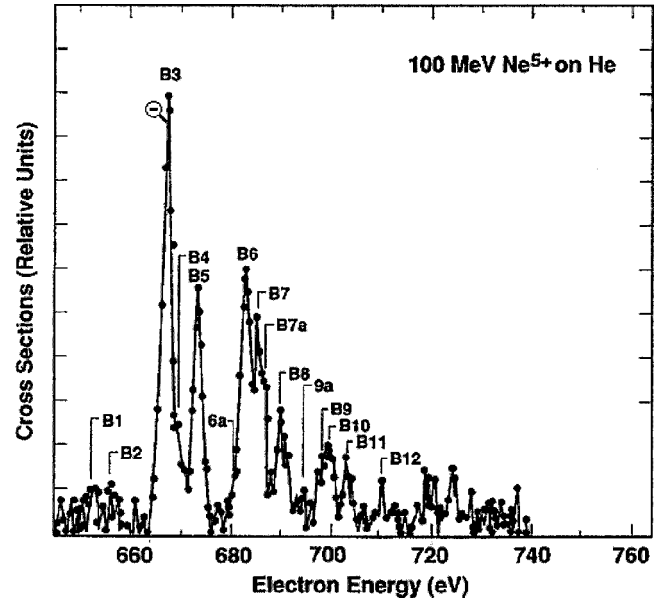


FIG. 3. High resolution zero-degree electron spectrum produced by 100-MeV Ne⁵⁺+He collisions. The spectrum is displayed after background subtraction and transformation to the projectile rest frame. The observed Auger lines arise mainly from Be-like core-excited 1s2s²2p and 1s2s2p² initial configurations. See also Ref. [10]. (From Ref. [7].)

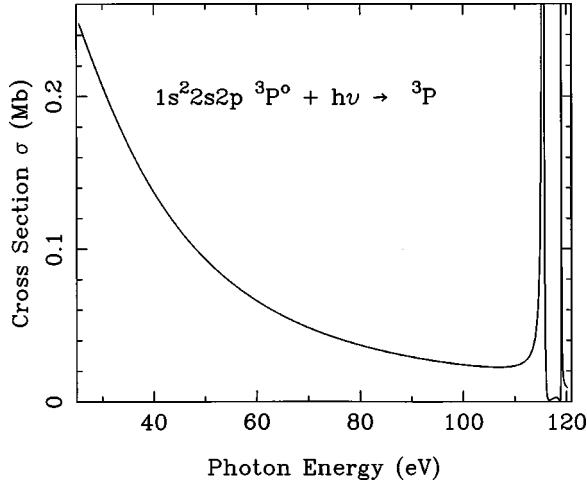
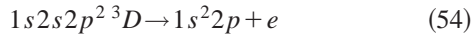
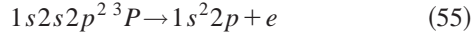


FIG. 4. The photoionization cross section near the resonance $1s^2 2s 2p^2 ^3P$. There are two peaks near 120 eV.

Peak A5 in the spectrum of the 100-MeV $\text{Ne}^{6+} + \text{He}$ collision is reported at 684.0 ± 0.4 eV. We identify this peak as a blend of two Auger channels

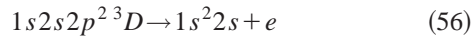


predicted at 684.36 eV and



predicted at 684.67 eV. This identification agrees with the theoretical results in Ref. [7]. We note that it disagrees with those of Kádár *et al.* [11] measured at 684.67 and 684.05 eV, respectively. In Ref. [7] the authors also identify the line B7 at 684 ± 0.2 eV as the transition (55), but in this work our prediction for transition (55) lies slightly higher than the uncertainty of the experiment.

The line B10 at 699.8 ± 0.4 eV is somewhat broad, and it was identified as from



and from $(1s^2 2s^2 2p^2)^2P$ [7]. Our results show that the actual 3D Auger energy is slightly higher at 700.39 eV. From Table XII, our result is close to the result of the $1/Z$ expansion but the deviation from the multiconfiguration Dirac-Fock calculation is somewhat larger.

In the comparison of the theoretical results in Table XII, it appears that the energy in the multiconfiguration Dirac-Fock calculation are usually the highest and that of the $1/Z$ expansion is the lowest for the seven lines listed. The energy of the Auger electron is usually higher than the experimental data in the multiconfiguration Dirac-Fock calculation, and lower than the experimental data in the $1/Z$ expansion calculation. However, the results of the saddle-point method agree with experiment very well for these resonances.

V. PHOTOIONIZATION FROM $\text{Be } ^3P^o$

In this work we compute the PICS from $\text{Be } 1s^2 2s 2p^2 ^3P^o$. We study the line profiles of the PICS near the four

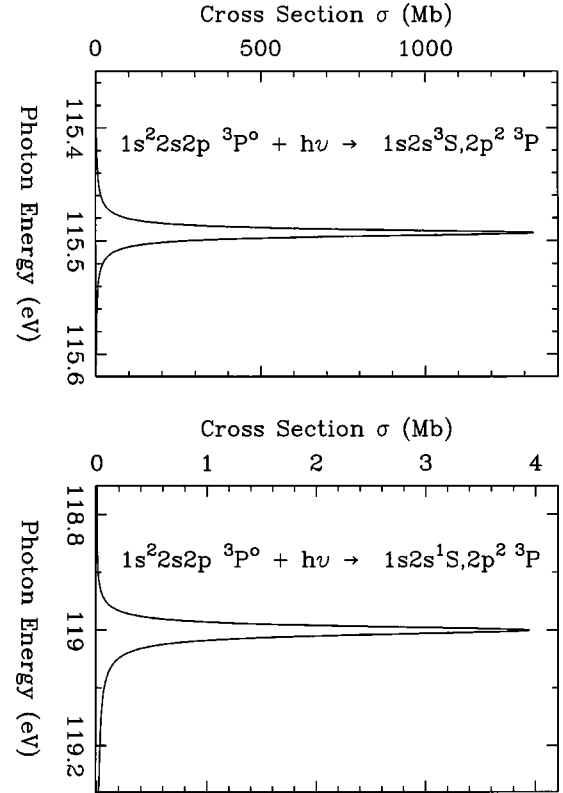


FIG. 5. The photoionization cross section near the resonance $1s^2 2s 2p^2 ^3P$. The left panel is for $(1s^2 s)^3S, 2p^2 ^3P$, and the right for $(1s^2 s)^1S, 2p^2 ^3P$. The peak PICS of the former is larger than that of the latter by a factor of more than 300.

resonance states, i.e., $1s^2 2s 2p^2 ^3S, 1s^2 2s 2p^2 ^3P(1)$, $1s^2 2s 2p^2 ^3P(2)$, and $1s^2 2s 2p^2 ^3D$. In this work, we use $-14.669\,677$ a.u. for the $\text{Be } 1s^2 2s^2$ energy [40]. The energy difference between the ground state and the lowest triplet state $1s^2 2s 2p^2 ^3P^o$ is 2.725 eV [41].

In this PICS calculation, we found that the cross sections are very small when away from resonances. Peaks occurred

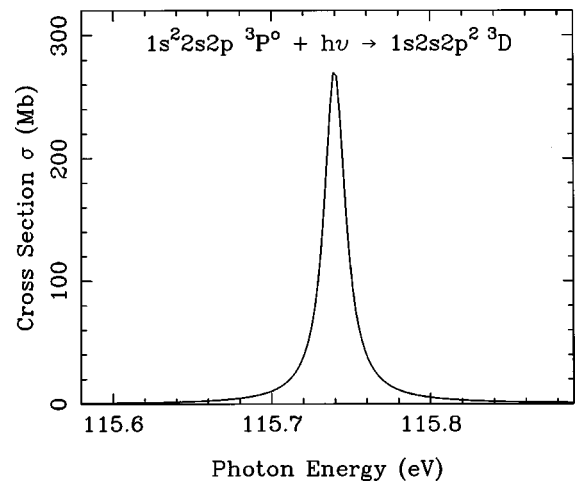


FIG. 6. The photoionization cross section near the resonance $1s^2 2s 2p^2 ^3D$.

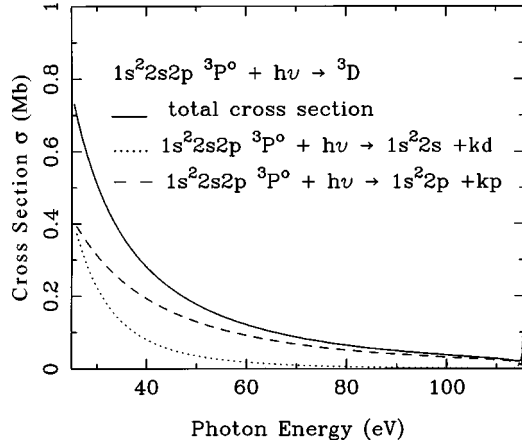


FIG. 7. The photoionization cross section near the resonance $1s2s2p^2\ ^3D$. The cross sections of two different channels are presented, and the total cross section is approximately the sum of the cross sections of these two channels.

in the region about 115 eV and 120 eV where two peaks show up within a region of about 5 eV. The first peak is centered at 115.5 eV. The cross section rises to about 1300 Mb from around 10^{-1} Mb (see Fig. 4 and Fig. 5). This peak comes from the $1s2s2p^2\ ^3P(1)$ resonance, i.e.,

$$1s^2 2s 2p\ ^3P^o + h\nu \rightarrow 1s2s2p^2\ ^3P(1). \quad (57)$$

Our prediction shows that this is a very strong peak. From our calculation for the $1s2s2p^2\ ^3P(1)$ state in the previous section, the energy is 10.325 346 a.u. Therefore, the difference between $1s^2 2s 2p\ ^3P^o$ and $1s2s2p^2\ ^3P(1)$ is 115.48 eV. This agrees with the PICS result obtained here. The second peak which occurs around 119 eV is significantly weaker. The peak cross section is only 4 Mb (see Fig. 5). It comes from the process

$$1s^2 2s 2p\ ^3P^o + h\nu \rightarrow 1s2s2p^2\ ^3P(2). \quad (58)$$

This also agrees with our previous calculation, which predicts the resonance to occur at 118.98 eV photon energy. The peak PICS of $1s2s2p^2\ ^3P(1)$ is larger than that of $1s2s2p^2\ ^3P(2)$ by a factor of more than 300.

In Fig. 6 and Fig. 7, the cross section is raised to 280 Mb. From Fig. 7, we see that the peak rises from a rather small background cross section. This resonance is due to

$$1s^2 2s 2p\ ^3P^o + h\nu \rightarrow 1s2s2p^2\ ^3D. \quad (59)$$

In Fig. 7 we combined cross sections from the different channels. Figure 8 shows the cross section near the resonance at 117.3 eV. This peak is about 40 Mb. It comes from the $1s2s2p^2\ ^3S$ resonance, i.e.,

$$1s^2 2s 2p\ ^3P^o + h\nu \rightarrow 1s2s2p^2\ ^3S. \quad (60)$$

VI. CONCLUSION

We have made an extensive study of triplet core-excited Be-like systems for Be I, B II, C III, N IV, O V, F VI, and

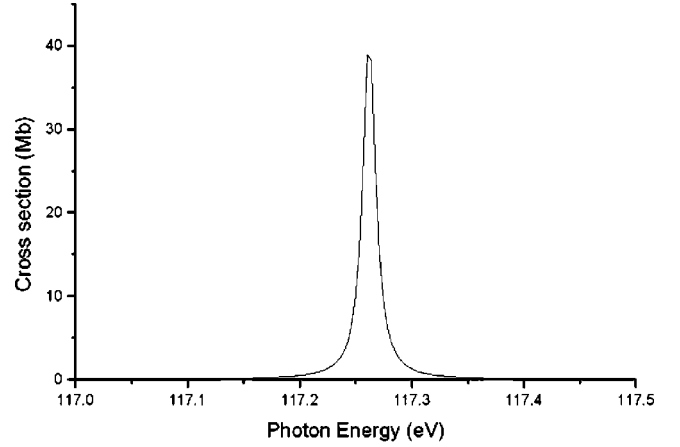


FIG. 8. The photoionization cross section for the resonance $1s2s2p^2\ ^3S$.

Ne VII. These results are used to identify the Auger lines coming from $1s2s^2 2p\ ^3P^o$ and $1s2s2p^2\ ^3S, ^3P^3D$ resonances in existing experimental spectra. The identification is made based not only on the calculated energy, but also on the predicted branching ratios. If the suggested identifications in this work are correct then the agreement between theory and experiment is excellent. Our results suggest that the saddle-point complex-rotation method is an accurate and powerful method for four-electron resonances. The branching ratios calculated in this work appear to support the Auger decay theory of Chung [25].

We have calculated the four-electron resonances for Be I through Ne VII. From these results, we can make a systematic isoelectronic study of these resonances and compare them with the observed spectra. We found that the similarity is striking within the isoelectronic series, and the intense lines in the observed spectra are all coming from the same resonances. The branching ratios are very similar for different Z . That means the interaction between electrons in the atom does not vary greatly with Z in the range $Z=4-10$.

For some of the theoretical results in this work, there are still no experimental data in the literature for comparison, especially for the photoionization. We hope these results will be useful in future experiments on Auger spectra and on photoionization. Our results also suggest possible overlap in the Auger spectra. We hope these data may help experimental workers in resolving the overlap resonances in the future.

ACKNOWLEDGMENTS

This work is supported by the National Science Council, Taiwan, R.O.C., Grant No. NSC 89-2112-M-007-008 and by the U.S. National Science Foundation. This work started while K.T.C. was visiting the National Center for Theoretical Science, at Tsing-Hua University, Hsin-Chu, Taiwan, supported by the National Science Council of Taiwan, Republic of China.

- [1] M. Rødbro, R. Bruch, and P. Bisgaard, *J. Phys. B* **12**, 2413 (1979).
- [2] R. Mann, *Phys. Rev. A* **35**, 4988 (1987).
- [3] R. Bruch, K. T. Chung, W. L. Luken, and J. C. Culberson, *Phys. Rev. A* **31**, 310 (1985).
- [4] K. T. Chung, *Phys. Rev. A* **41**, 4090 (1990).
- [5] R. Bruch, N. Stolterfoht, S. Datz, P. D. Miller, P. L. Pepmiller, Y. Yamazaki, H. F. Krause, J. K. Swenson, K. T. Chung, and B. F. Davis, *Phys. Rev. A* **35**, 4114 (1987).
- [6] R. Bruch, D. Schneider, M. H. Chen, K. T. Chung, and B. F. Davis, *Phys. Rev. A* **45**, 4476 (1992).
- [7] R. Bruch, D. Schneider, M. H. Chen, K. T. Chung, and B. F. Davis, *Phys. Rev. A* **44**, 5659 (1991).
- [8] R. Bruch, D. Schneider, W. H. E. Schwarz, M. Meinhart, B. M. Johnson, and K. Taulbjerg, *Phys. Rev. A* **19**, 587 (1979).
- [9] R. Bruch, S. Datz, P. D. Miller, P. L. Pepmiller, H. F. Krause, J. K. Swenson, and N. Stolterfoht, *Phys. Rev. A* **36**, 394 (1987).
- [10] A. Itoh, D. Schneider, T. Schneider, T. Y. M. Zouros, G. Nolte, A. Schiwietz, W. Zeitz, and N. Stolterfoht, *Phys. Rev. A* **31**, 684 (1985).
- [11] I. Kádár, S. Ricz, J. Végh, B. Sulik, D. Varga, and D. Berényi, *Phys. Rev. A* **41**, 3518 (1990).
- [12] P. G. Burke, J. W. Cooper, and S. Ormonde, *Phys. Rev.* **183**, 245 (1969); W. C. Fon *et al.*, *J. Phys. B* **11**, 325 (1978).
- [13] R. K. Nesbet, *Phys. Rev. A* **12**, 444 (1975).
- [14] A. Temkin, A. K. Bhatia, and J. N. Bardsley, *Phys. Rev. A* **5**, 1663 (1972); A. Temkin and A. K. Bhatia, in *Autoionization—Recent Developments and Applications*, edited by A. Temkin (Plenum, New York, 1985), Chap. 2.
- [15] L. Voky, H. E. Saraph, W. Eissner, Z. W. Liu, and H. P. Kelly, *Phys. Rev. A* **46**, 3945 (1992).
- [16] H. P. Saha and C. D. Caldwell, *Phys. Rev. A* **40**, 7020 (1989).
- [17] E. W. B. Dias, H. S. Chakraborty, P. C. Deshmukh, and S. T. Manson, *J. Phys. B* **32**, 3383 (1999).
- [18] K. T. Chung, *Phys. Rev. A* **20**, 1743 (1979).
- [19] K. T. Chung and B. F. Davis, in *Autoionization—Recent Developments and Applications* (Ref. [14]), Chap. 3; B. F. Davis and K. T. Chung, *Phys. Rev. A* **37**, 111 (1988); B. Jaskoska and W. Woznicki, *Phys. Scr.* **39**, 230 (1989).
- [20] K. T. Chung, *J. Phys. B* **23**, 2929 (1990).
- [21] K. T. Chung, *Phys. Scr.* **42**, 530 (1990).
- [22] K. T. Chung, *Phys. Scr.* **42**, 537 (1990).
- [23] K. T. Chung, *Phys. Rev. A* **42**, 645 (1990).
- [24] K. T. Chung, *Chin. J. Phys. (Taipei)* **27**, 507 (1989).
- [25] K. T. Chung, *Phys. Rev. A* **59**, 2065 (1999).
- [26] K. T. Chung and X.-W. Zhu, *Phys. Scr.* **44**, 292 (1993).
- [27] E. Balslev and J. M. Combes, *Commun. Math. Phys.* **22**, 280 (1971).
- [28] K. T. Chung and B. F. Davis, *Phys. Rev. A* **26**, 3278 (1982).
- [29] B. R. Junker and C. L. Huang, *Phys. Rev. A* **18**, 313 (1978).
- [30] B. Simon, *Commun. Math. Phys.* **27**, 1 (1972).
- [31] K. T. Chung, *Phys. Rev. Lett.* **78**, 1416 (1997).
- [32] T. N. Rescigno and V. McKoy, *Phys. Rev. A* **12**, 522 (1975).
- [33] A. Dalgarno and J. T. Lewis, *Proc. R. Soc. London, Ser. A* **233**, 70 (1955).
- [34] K. T. Chung, *Phys. Rev. A* **44**, 5421 (1991).
- [35] Z.-W. Wang, X.-W. Zhu, and K. T. Chung, *Phys. Scr.* **47**, 65 (1993).
- [36] S. Bashkin and J. O. Stoner, Jr., *Atomic Energy Levels and Grottrian Diagrams* (North-Holland Publishing Co., New York, 1975).
- [37] U. I. Safronova and V. N. Kharitonova, *Opt. Spectrosc.* **27**, 300 (1969).
- [38] K. T. Chung and R. Bruch, *Phys. Rev. A* **28**, 1418 (1983).
- [39] M. H. Chen, *Phys. Rev. A* **31**, 1449 (1985).
- [40] K. T. Chung, X.-W. Zhu, and Z.-W. Wang, *Phys. Rev. A* **47**, 1740 (1993).
- [41] K. T. Chung and X.-W. Zhu, *Phys. Rev. A* **48**, 1944 (1993).
- [42] S. Schumann, K. O. Groeneveld, A. Nolte, and B. Fricke, *Z. Phys. A* **289**, 245 (1979).